

within the LinDistFlow-based flexibility set. This intuitive approach is both effective and computationally efficient, while preserving privacy by preventing the disclosure of detailed distribution grid information.

- Beyond tutorial examples, we extend the simulations to coordinated integrated transmission-distribution (ITD) systems, focusing on the impact of electricity price variations and scenarios involving multiple distribution systems. The results validate the proposed compensation method's ability to improve accuracy with minimal additional computational effort.

The remainder of this article is structured as follows: Section II introduces the power system model and the concept of coordination using the flexibility set. Section III presents the flexibility aggregation methods based on the LinDistFlow model and the proposed system loss compensation approach, illustrated with tutorial examples. Section IV provides more extensive simulations to evaluate the proposed methods. Finally, Section V concludes the paper.

II. PROBLEM STATEMENT

Consider a power grid modeled as integrated transmission-distribution (ITD) system, represented by the tuple $(\mathcal{N}, \mathcal{L}, \mathcal{S})$, where \mathcal{N} represents the set of buses, \mathcal{L} represents the set of branches, and \mathcal{S} represents the set of subsystems, which include both transmission and distribution systems, i.e., $\mathcal{S} = \mathcal{S}^T \cup \mathcal{S}^D$.

In this paper, we focus on a single transmission system, i.e., $|\mathcal{S}^T| = 1$, connected with multiple radial distribution systems, i.e., $|\mathcal{S}^D| \geq 1$. We assign the transmission system an index of 1, i.e., $\mathcal{S} = \{1\}$. Each subsystem $\xi \in \mathcal{S}$ is represented as a directed graph $(\mathcal{N}_\xi, \mathcal{L}_\xi)$, where \mathcal{N}_ξ and \mathcal{L}_ξ denote the set of buses and branches within the subsystem ξ , respectively. For every radial distribution subsystem $\xi \in \mathcal{S}^D$, the number of buses N_ξ^{bus} and branches N_ξ^{line} are related by $N_\xi^{\text{bus}} = N_\xi^{\text{line}} + 1$. The power generation in the distribution systems refers to the controllable power output of distributed energy resources (DERs).

The transmission and each distribution system are interconnected at a point of common coupling (PCC), typically located at distribution substations corresponding to the first bus in the local bus set \mathcal{N}_ξ . In this paper, we assume that the voltage magnitude at the PCC is fixed by the substations and is independent of the transmission system voltage.

A. Model of Transmission Systems

In the transmission system ($\xi = 1$), the complex voltage at a bus $i \in \mathcal{N}_1$ is expressed in polar coordinates, i.e., $V_i = v_i e^{j\theta_i}$, where v_i and θ_i are the magnitude and angle of the complex voltage V_i . Thereby, the classic AC model of the transmission

system can be written as follows

$$p_i^g - p_i^\xi = v_i \sum_{k \in \mathcal{N}} v_k (g_{ik} \cos \theta_{ik} + b_{ik} \sin \theta_{ik}), \forall i \in \mathcal{N}_1 \quad (1a)$$

$$q_i^g - q_i^\xi = v_i \sum_{k \in \mathcal{N}} v_k (g_{ik} \sin \theta_{ik} - b_{ik} \cos \theta_{ik}), \forall i \in \mathcal{N}_1 \quad (1b)$$

$$v_i \leq v_i \leq \bar{v}_i, \quad \underline{p}_i^g \leq p_i^g \leq \bar{p}_i^g, \quad \underline{q}_i^g \leq q_i^g \leq \bar{q}_i^g, \forall i \in \mathcal{N}_1 \quad (1c)$$

where p_i^g and q_i^g (resp. p_i^ξ and q_i^ξ) denote the real and reactive power produced by generators (resp. send to distribution system ξ) at bus i . These variables are set to 0 if no generator (resp. distribution system) is connected to a bus i . The parameters g, b denote the real and imaginary part of the complex nodal admittance matrix Y . The signs $\underline{\cdot}$ and $\bar{\cdot}$ denote upper and lower bounds for the corresponding state variables.

B. Model of Distribution Systems

In the following, we introduce two models for the distribution system: the DistFlow model [12], [13] and the LinDistFlow model [11]. Both models are formulated using squared voltage coordinates, i.e., $U_i = |V_i|^2, \forall i \in \mathcal{N}_\xi$.

Remark 1 ([19]). *The DistFlow model can be interpreted as an angle relaxation of the classical AC model (1), and the angle relaxation is exact when the distribution network is radial.*

Remark 2. *In the present paper, when we state that an approximation or relaxation is exact, we mean that the model produces results identical to those of the AC power flow model (1).*

For clarity, we omit the subsystem index ξ in the variables, as all variables belong to the same distribution system ξ . Furthermore, the system models are reformulated in matrix form for the methods introduced in the following section. Details on the connectivity matrices C^t, C^f , and C^g can be found in [20], with the incidence matrix defined as $C = C^f - C^t$.

1) DistFlow Model

The DistFlow model can be written in a matrix form:

$$0 = e_1^\top U - 1 \quad (2a)$$

$$0 = C U - 2(\mathbf{R}P_l + \mathbf{X}Q_l) + (\mathbf{R}^2 + \mathbf{X}^2) L \quad (2b)$$

$$0 = C^\top P_l + (C^t)^\top \mathbf{R} L - e_1^\top p^{\text{pcc}} - C^g p^g + P^d \quad (2c)$$

$$0 = C^\top Q_l + (C^t)^\top \mathbf{X} L - e_1^\top q^{\text{pcc}} - C^g q^g + Q^d \quad (2d)$$

$$0 = \mathbf{U} L - (\mathbf{P}^2 + \mathbf{Q}^2) \quad (2e)$$

$$\underline{U} \leq U \leq \bar{U}, \quad \underline{p}^{\text{pcc}} \leq p^{\text{pcc}} \leq \bar{p}^{\text{pcc}}, \quad \underline{q}^{\text{pcc}} \leq q^{\text{pcc}} \leq \bar{q}^{\text{pcc}} \quad (2f)$$

$$\underline{p}^g \leq p^g \leq \bar{p}^g, \quad \underline{q}^g \leq q^g \leq \bar{q}^g \quad (2g)$$

with

$$\begin{aligned} \mathbf{P} &= \text{diag}(P_l), & \mathbf{Q} &= \text{diag}(Q_l), & \mathbf{U} &= \text{diag}(C U), \\ \mathbf{R} &= \text{diag}(R), & \mathbf{X} &= \text{diag}(X), \end{aligned}$$

where $e_1 = [1, 0, \dots, 0]^\top \in \mathbb{R}^{N^{\text{bus}}}$, and $U \in \mathbb{R}^{N^{\text{bus}}}$ stacks squared voltage magnitudes for all buses in \mathcal{N} . The vectors $L, P_l, Q_l, X, R \in \mathbb{R}^{N^{\text{line}}}$ represents stacked squared current

magnitude l_{ij} and power flows p_{ij} , q_{ij} , resistance r_{ij} and reactance x_{ij} of branch $(i, j) \in \mathcal{L}_\xi$, respectively. The vectors P^g and Q^g (resp. P^d and Q^d) denote vectors stacked with the active and reactive generation injections of controllable devices (resp. demands, i.e., consumption by customer). p^{pcc} and q^{pcc} denote active and reactive power injections via PCC from a transmission system.

Additionally, due to power conservation in the subsystem ξ , we have:

$$p^{\text{pcc}} + \sum_{i \in \mathcal{N}_\xi} p_i^g - \sum_{i \in \mathcal{N}_\xi} p_i^d - R^\top L = 0, \quad (3a)$$

$$q^{\text{pcc}} + \sum_{i \in \mathcal{N}_\xi} q_i^g - \sum_{i \in \mathcal{N}_\xi} q_i^d - X^\top L = 0. \quad (3b)$$

2) LinDistFlow Model

The LinDistFlow model can be expressed in matrix form as:

$$0 = e_1^\top U - 1 \quad (4a)$$

$$0 = CU - 2(RP_l + XQ_l) \quad (4b)$$

$$0 = C^\top P_l - e_1 p^{\text{pcc}} - C^g p^g + P^d \quad (4c)$$

$$0 = C^\top Q_l - e_1 q^{\text{pcc}} - C^g q^g + Q^d \quad (4d)$$

$$\underline{U} \leq U \leq \bar{U}, \underline{p}^{\text{pcc}} \leq p^{\text{pcc}} \leq \bar{p}^{\text{pcc}}, \underline{q}^{\text{pcc}} \leq q^{\text{pcc}} \leq \bar{q}^{\text{pcc}} \quad (4e)$$

$$\underline{p}^g \leq p^g \leq \bar{p}^g, \underline{q}^g \leq q^g \leq \bar{q}^g \quad (4f)$$

Remark 3 (Lossless Approximation). The LinDistFlow (4) is derived by omitting higher-order power loss terms in (2b)(2c)(2d), i.e., setting $l_{ij} = 0$ for all branches $(i, j) \in \mathcal{L}_\xi$. This omission also removes the quadratic constraint (2e), making LinDistFlow a linearized version of the DistFlow model (2) that ignores power losses.

C. Optimal Power Flow for ITD Systems

To ensure consistency, the power injected into the system at the PCC must equal the power supplied from the transmission system at the corresponding bus i , as expressed by:

$$p_\xi^{\text{pcc}} = p_i^\xi, \quad q_\xi^{\text{pcc}} = q_i^\xi, \quad (5)$$

where $i \in \mathcal{N}_1$. The objective is to minimize the overall power generation cost defined as

$$\sum_{i \in \mathcal{N}} c_{i,2} (p_i^g)^2 + c_{i,1} p_i^g + c_{i,0} \quad (6)$$

where $a_{i,2}$, $a_{i,1}$, and $a_{i,0}$ denote the cost coefficients of operation cost of power generations at bus i .

The optimal power flow (OPF) problems for the ITD systems can be written as

$$\min (6) \quad (\text{Generation Cost}) \quad (7a)$$

$$\text{s.t. (1),} \quad (\text{Trans. Constraints}) \quad (7b)$$

$$(2), \forall \xi \in \mathcal{S}^D, \quad (\text{Distr. Constraints}) \quad (7c)$$

$$(5), \forall \xi \in \mathcal{S}^D \quad (\text{Power Exchange}) \quad (7d)$$

The solutions to (7) are exact when all distribution networks are radial, as noted in Remark 1.

Flexibility aggregation methods are employed to define a feasible region \mathcal{U}^ξ for each distribution system $\xi \in \mathcal{S}^D$. This allows the optimization problem (7) to be reformulated as:

$$\min (6) \quad (8a)$$

$$\text{s.t. (1),} \quad (8b)$$

$$(p_\xi^{\text{pcc}}, q_\xi^{\text{pcc}}) \in \mathcal{U}^\xi, \forall \xi \in \mathcal{S}^D, \quad (8c)$$

so that detailed constraints for distribution systems (7c) are no longer required.

III. FLEXIBILITY AGGREGATION METHODS

In this section, we begin by discussing flexibility aggregation methods based on the LinDistFlow model (4). We then illustrate the challenges associated with these methods and introduce an intuitive compensation approach based on the properties of the model with tutorial examples. Similar to Section II-B, we omit the subsystem index ξ in this section.

A. Flexibility Aggregation based on LinDistFlow Model

The LinDistFlow models (4) can be reformulated as follows:

$$Ax + Bu - b = 0, \quad \underline{x} \leq x \leq \bar{x}, \quad \underline{u} \leq u \leq \bar{u} \quad (9)$$

with

$$A = \begin{bmatrix} e_1^\top & 0 & 0 & 0 & 0 \\ C & -2R & -2X & 0 & 0 \\ 0 & -C^\top & 0 & C^g & 0 \\ 0 & 0 & -C^\top & 0 & C^g \end{bmatrix}, \quad B = \begin{bmatrix} 0 & 0 \\ 0 & 0 \\ e_1 & 0 \\ 0 & e_1 \end{bmatrix},$$

$$x^\top = [U^\top \quad (P^l)^\top \quad (Q^l)^\top \quad p^g \quad q^g],$$

$$u^\top = [p_{\text{pcc}} \quad q_{\text{pcc}}]^\top \text{ and } b = [e_1^\top \quad 0 \quad (P^d)^\top \quad (Q^d)^\top].$$

Proposition 1 (Prop. 1 in [4]). Given a radial network, matrix A is invertible.

Remark 4. This paper focuses on improving flexibility aggregation methods to address the challenges of nonlinearity in the AC model. Benchmarks used in this paper are limited to a single DER with controllable active and reactive power injections in one distribution system. For systems with multiple controllable DER, participation factors, as used in system balancing [21], are recommended to ensure invertibility to the matrix A .

The task in flexibility aggregation is to propagate the constraints on x , through the grid and map them onto the active and reactive power exchange u at the PCC. For the LinDistFlow model (9), since the matrix A is invertible, all state variables x can be explicitly expressed in terms of u as follows:

$$x = A^{-1} (b - Bu), \quad (10)$$

and the resulting flexibility set can be expressed as

$$\mathcal{U}_{\text{LDS}} = \{u \mid \underline{x} \leq A^{-1} (b - Bu) \leq \bar{x}, \quad \underline{u} \leq u \leq \bar{u}\}.$$

However, omitting power losses (Remark 3) introduces errors in the system. Compared to other applications, such as local voltage control strategies [22], aggregating the flexibility in

a distribution system requires defining a broader set at the PCC. Moreover, all line losses are effectively accumulated at $(p^{\text{pcc}}, q^{\text{pcc}})$, causing the errors introduced by the LinDistFlow model to propagate into the resulting flexibility set \mathcal{U}_{LDS} .

To illustrate this, three tutorial examples, i.e., case10ba, case33mg, and case118zh from MATPOWER [23], are shown in Fig. 2. The topologies of these examples are presented in the first row of Fig. 2, demonstrating that all DERs are connected to one of the leaf nodes, thereby accumulating all line losses along the path to the root node.

Fig. 2f, Fig. 2d, and Fig. 2e depict the exact flexibility sets bounded by voltage limits (blue lines), active power limits (red lines), and reactive power limits (purple lines). Solid lines represent the upper bounds, while dashed lines correspond to the lower bounds. The red region represents the LinDistFlow-based flexibility set \mathcal{U}_{LDS} . Notably, the flexibility set \mathcal{U}_{LDS} exhibits relatively large errors due to the accumulation of losses, and these errors grow as the system size increases.

B. System Loss Compensation

To address the errors introduced by the LinDistFlow model, we propose an intuitive approach to compensate for system losses inspired by power conservation (3). To simplify computation, we first introduce the following assumption:

Assumption 1. *We assume that the voltage difference across branches remains constant within the flexibility set \mathcal{U} .*

The main idea is to first determine the LinDistFlow-based flexibility set \mathcal{U}_{LDS} , as described in Section III-A. Since all state variables x can be expressed as a linear mapping from u via (10), we have:

$$\mathbf{P}(u) = \text{diag}(\bar{A}_p u + \bar{b}_p) \quad (11a)$$

$$\mathbf{Q}(u) = \text{diag}(\bar{A}_q u + \bar{b}_q) \quad (11b)$$

where \bar{A}_p, \bar{A}_q and \bar{b}_p, \bar{b}_q are constructed from the corresponding rows of $-A^{-1}B$ and $A^{-1}b$ in (10).

With Assumption 1, system losses can be efficiently computed as quadratic functions of u :

$$p^{\text{loss}}(u) = R^\top \hat{\mathbf{U}}^{-1} (\mathbf{P}^2(u) + \mathbf{Q}^2(u)) \mathbf{1}, \quad (12a)$$

$$q^{\text{loss}}(u) = X^\top \hat{\mathbf{U}}^{-1} (\mathbf{P}^2(u) + \mathbf{Q}^2(u)) \mathbf{1}, \quad (12b)$$

where $\mathbf{1} \in \mathbb{R}^{N^{\text{line}}}$ denotes the vector of all ones, and $\hat{\mathbf{U}} = \text{diag}(C \hat{\mathbf{U}}) = \text{diag}(C^f \hat{\mathbf{U}} - C^t \hat{\mathbf{U}})$ represents an estimate of the squared voltage differences. In this paper, we compute $\hat{\mathbf{U}}$ by setting $p^g = q^g = 0$. Alternatively, the losses can be reformulated as:

$$p^{\text{loss}}(u) = \frac{1}{2} u^\top H_p u + g_p^\top u + c_p, \quad (13a)$$

$$q^{\text{loss}}(u) = \frac{1}{2} u^\top H_q u + g_q^\top u + c_q. \quad (13b)$$

with $H_p, H_q \in \mathbb{R}^{2 \times 2}$, $g_p, g_q \in \mathbb{R}^2$ and $c_p, c_q \in \mathbb{R}$.

Remark 5 (Data Privacy). *The quadratic functions $p^{\text{loss}}(\cdot), q^{\text{loss}}(\cdot)$ accumulate estimated losses across all*

branches. As a result, transmitting $H_p, H_q, g_p, g_q, c_p, c_q$ does not reveal sensitive data.

The flexibility set with system loss compensation can then be written as:

$$\mathcal{U}_{\text{SLC}} = \left\{ u \mid u = u_{\text{LDS}} + \begin{bmatrix} p^{\text{loss}}(u_{\text{LDS}}) \\ q^{\text{loss}}(u_{\text{LDS}}) \end{bmatrix}, u_{\text{LDS}} \in \mathcal{U}_{\text{LDS}} \right\}.$$

The effectiveness of the proposed compensation is illustrated in Fig. 2. The flexibility sets with system loss compensation \mathcal{U}_{SLC} are shown as the green regions in the subfigures of the second row. Compared to the original LinDistFlow-based flexibility set \mathcal{U}_{LDS} , the compensation significantly improves the approximation of the exact flexibility set. Although some violations exist—such as the upper-right corner of for example, the upper-right corner of \mathcal{U}_{SLC} in Fig. 2f and relatively large deviations near lower voltage limits—these may result from the constant voltage difference assumption (Assumption 1) used for computational efficiency. Nevertheless, the compensation provides a good approximation for power limits.

IV. SIMULATION

We evaluate our loss compensation approach through numerical simulations of a coordination problem. Specifically, we assess the solution quality by solving the flexibility optimization problem (7) for distribution systems using both the LinDistFlow-based flexibility aggregation and the proposed loss compensation method. The results are compared to those of the original optimization problem (8).

The simulations include two scenarios: the first involves a single DSO with varying generation costs, while the second addresses a coordination problem with 29 distribution systems. We use radial distribution networks provided by MATPOWER as the test systems, each equipped with a distributed energy resource (DER). A controllable DER is placed at a leaf node in each network, as shown in Fig. 2. The power bounds of the DERs are set as fixed percentages of the total demand.

A. Performance with Different Cost

To evaluate coordination with aggregated flexibility (8) under various scenarios, we first consider the TSO connected to a single DSO. We simulate three different cases by choosing three distribution grids, namely case118zh, case10ba, and case33mg. In electricity markets, prices fluctuate over time, and we simulate different coordination scenarios by varying the cost parameters of the DSO, ranging from lower to higher than those of the TSO. For each scenario, the corresponding power injection at the PCC is recorded.

As a reference for comparison, dispatch points are first calculated solving the centralized coordination problem (7), where the TSO is modeled with the AC power flow model, and the DSO is modeled with the DistFlow model. These results, marked as blue crosses in Fig. 2i-Fig. 2h, are arranged from left to right, corresponding to increasing prices.

Next, we solve the coordination problem with aggregated flexibility (8). When using the LinDistFlow model, the results are marked as red rectangles. Because the LinDistFlow model

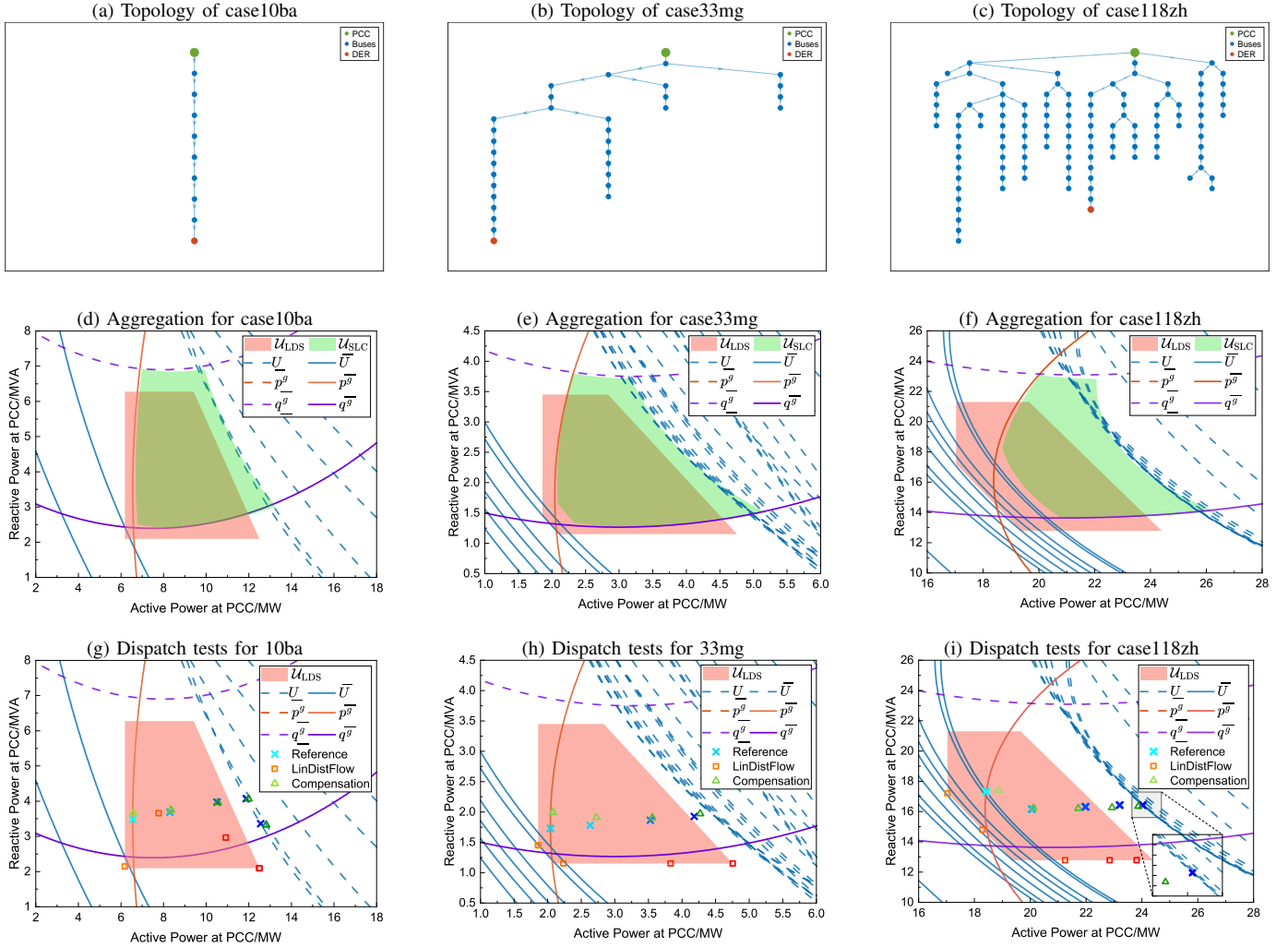


Figure 2: First row: The topology of the radial networks, with DER location and PCC. Second row: Shaded regions represent the LinDistFlow model (red) (i) and the compensation method (green) (ii). Dashed and solid lines mark the exact flexibility bounds, derived from solutions using DistFlow model. Third row: Markers show PCC power flows for different costs, increasing in price from left to right.

neglects power losses, these dispatch points are positioned at the boundaries of the exact flexibility region, violating the limits established by the DistFlow model. However, applying the compensation method corrects for these power losses by adding them to the power flow at the PCC. The resulting dispatch points, marked as green triangles, align closely with the reference points, demonstrating the effectiveness of the compensation method.

B. Overall Performance with Multiple Distribution Systems

In the scenarios discussed above, the compensation method demonstrates that decentralized coordination can closely approximate the exact dispatch decisions. Now, we consider a more complex scenario where multiple networks are interconnected. This merged system consists of a transmission network (case30) and three types of distribution networks—case118zh, case10ba, and case33mg—operated by DSOs, following the configurations described above. The connectivity matrix C_{PCC} is constructed by sorting the active demands in case30: nodes with demands exceeding 15 MW are connected to case118zh,

those between 5 MW and 15 MW to case10ba, and those below 5 MW to case33mg, as illustrated in Fig. 1.

Decentralized coordination determines only the power flow at the TSO-DSO interface, leaving the internal states of the distribution networks unresolved. To address this, each DSO must perform a post-coordination calculation, solving a power flow problem using the fixed power at the PCC as input. It ensures that DERs within the networks are scheduled appropriately and provides operational data for the DSOs.

The results of the post-coordination calculation, summarized in Fig. 3, demonstrate significant improvements in coordination accuracy achieved by the loss compensation method compared to the LinDistFlow model. In Fig. 3b, we can see that the compensation method effectively reduces cost f discrepancies across all networks, aligning closely with centralized coordination cost f^* . In contrast, the LinDistFlow model exhibits larger cost deviations, as depicted in Fig. 3a. In particular, the case33mg, which is more sensitive to power losses due to its smaller size and lower demand, shows large cost deviations. This sensitivity underscores the limitations

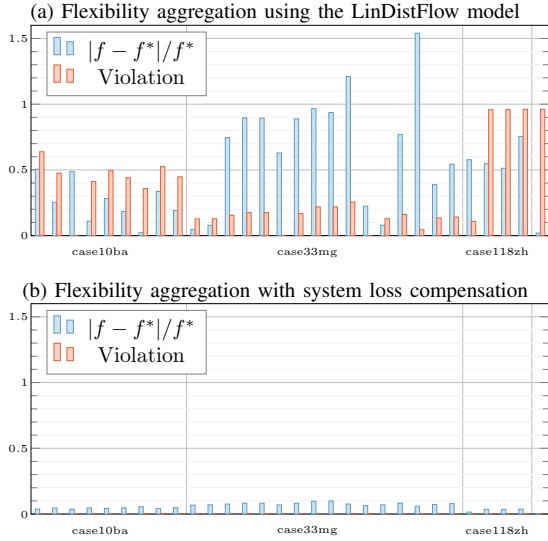


Figure 3: Performance of aggregating flexibility in a distribution system, considering one TSO connected with 29 distribution systems, including 9 case10ba, 16 case33mg and 4 case118zh

of the LinDistFlow model in accurately reflecting network characteristics under such conditions.

Additionally, the state variables within the distribution networks are resolved during the post-coordination calculation. Using the compensation method ensures that these variables remain within physical constraints, leading to no violations in Fig. 3b. In contrast, the results in Fig. 3a highlight the violations that occur when using the LinDistFlow model. Voltage lower-bound violations are consistent with expected behavior when DERs attempt to meet more demand, as higher voltage magnitudes are required. Reactive power constraints emerge as the most frequently violated limits, underscoring the critical role of reactive power in maintaining efficient power transmission and stable voltage levels.

V. CONCLUSION

The present paper analyzes the limitations of the LinDistFlow model for flexibility aggregation, highlighting its inherent approximation errors in both flexibility aggregation and TSO-DSO coordination. To address these issues, we propose a loss compensation method that leverages the computational efficiency of the LinDistFlow model while enhancing its accuracy for aggregation and coordination tasks. Simulation results demonstrate that the proposed method significantly reduces infeasibility and aligns more closely with reference solutions, thereby improving the practicality of LinDistFlow-based aggregation.

REFERENCES

- [1] D. K. Molzahn, F. Dörfler, H. Sandberg, S. H. Low, S. Chakrabarti, R. Baldick, and J. Lavaei, "A survey of distributed optimization and control algorithms for electric power systems," *IEEE Trans. Smart Grid*, vol. 8, no. 6, pp. 2941–2962, 2017.
- [2] N. Patari, V. Venkataramanan, A. Srivastava, D. K. Molzahn, N. Li, and A. Annaswamy, "Distributed optimization in distribution systems: Use cases, limitations, and research needs," *IEEE Trans. Power Syst.*, vol. 37, no. 5, pp. 3469–3481, 2021.
- [3] U. Cali, S. N. G. Gourisetti, D. J. Sebastian-Cardenas, F. O. Catak, A. Lee, L. M. Zeger, T. S. Ustun, M. F. Dnyge, S. Rao, and J. E. Ramirez, "Emerging technologies for privacy preservation in energy systems," in *European Interdisciplinary Cybersecurity Conference*, 2024, pp. 163–170.
- [4] X. Dai, Y. Guo, Y. Jiang, C. N. Jones, G. Hug, and V. Hagenmeyer, "Real-time coordination of integrated transmission and distribution systems: Flexibility modeling and distributed NMPC scheduling," *Electr. Power Syst. Res.*, vol. 234, p. 110627, 2024.
- [5] J. L. Mathieu, G. Verbič, T. Morstyn, M. Almassalkhi, K. Baker, J. Braslavsky, K. Bruninx, Y. Dvorkin, G. S. Ledva, N. Mahdavi *et al.*, "A new definition of demand response in the distributed energy resource era," *arXiv preprint arXiv:2410.18768*, 2024.
- [6] T. Zhang, J. Wang, H. Wang, J. Ruiyang, G. Li, and M. Zhou, "On the Coordination of Transmission-Distribution Grids: A Dynamic Feasible Region Method," *IEEE Trans. Power Syst.*, vol. 38, no. 2, pp. 1857–1868, Mar. 2023.
- [7] Y. Wen, Z. Hu, S. You, and X. Duan, "Aggregate feasible region of DERs: Exact formulation and approximate models," *IEEE Trans. Smart Grid*, vol. 13, no. 6, pp. 4405–4423, 2022.
- [8] Z. Tan, H. Zhong, Q. Xia, C. Kang, X. S. Wang, and H. Tang, "Estimating the Robust P-Q Capability of a Technical Virtual Power Plant Under Uncertainties," *IEEE Trans. Power Syst.*, vol. 35, no. 6, pp. 4285–4296, Nov. 2020.
- [9] L. Lopez, A. Gonzalez-Castellanos, D. Pozo, M. Roozbehani, and M. Dahleh, "QuickFlex: A Fast Algorithm for Flexible Region Construction for the TSO-DSO Coordination," in *2021 International Conference on Smart Energy Systems and Technologies (SEST)*. Vaasa, Finland: IEEE, Sep. 2021, pp. 1–6.
- [10] Y. Wen, Z. Hu, J. He, and Y. Guo, "Improved inner approximation for aggregating power flexibility in active distribution networks and its applications," 2023.
- [11] M. E. Baran and F. F. Wu, "Network reconfiguration in distribution systems for loss reduction and load balancing," *IEEE Trans. Power Deliv.*, vol. 4, no. 2, pp. 1401–1407, 1989.
- [12] —, "Optimal capacitor placement on radial distribution systems," *IEEE Trans. Power Deliv.*, vol. 4, no. 1, pp. 725–734, 1989.
- [13] M. Baran and F. F. Wu, "Optimal sizing of capacitors placed on a radial distribution system," *IEEE Trans. Power Deliv.*, vol. 4, no. 1, pp. 735–743, 1989.
- [14] S. Riaz and P. Mancarella, "On Feasibility and Flexibility Operating Regions of Virtual Power Plants and TSO/DSO Interfaces," in *2019 IEEE Milan PowerTech*. Milan, Italy: IEEE, 2019, pp. 1–6.
- [15] D. A. Contreras and K. Rudion, "Verification of Linear Flexibility Range Assessment in Distribution Grids," in *2019 IEEE Milan PowerTech*. Milan, Italy: IEEE, 2019, pp. 1–6.
- [16] J. Silva, J. Sumaili, R. J. Bessa, L. Seca, M. A. Matos, V. Miranda, M. Caujolle, B. Goncer, and M. Sebastian-Viana, "Estimating the Active and Reactive Power Flexibility Area at the TSO-DSO Interface," *IEEE Trans. Power Syst.*, vol. 33, no. 5, pp. 4741–4750, 2018.
- [17] S. Wang, W. Wu, Q. Chen, J. Yu, and P. Wang, "Stochastic Flexibility Evaluation for Virtual Power Plants by Aggregating Distributed Energy Resources," *CSEE JOURNAL OF POWER AND ENERGY SYSTEMS*, vol. 10, no. 3, 2024.
- [18] M. Kalantar-Neyestanaki, F. Sossan, M. Bozorg, and R. Cherkaoui, "Characterizing the Reserve Provision Capability Area of Active Distribution Networks: A Linear Robust Optimization Method," *IEEE Trans. Smart Grid*, vol. 11, no. 3, pp. 2464–2475, 2020.
- [19] M. Farivar and S. H. Low, "Branch flow model: Relaxations and convexification (Parts I, II)," *IEEE Trans. Power Syst.*, vol. 28, no. 3, pp. 2554–2564, 2013.
- [20] R. D. Zimmerman, C. E. Murillo-Sánchez, and R. J. Thomas, "Matpower: Steady-state operations, planning, and analysis tools for power systems research and education," *IEEE Trans. Power Syst.*, vol. 26, no. 1, pp. 12–19, 2010.
- [21] D. Lee, K. Turitsyn, D. K. Molzahn, and L. A. Roald, "Robust ac optimal power flow with robust convex restriction," *IEEE Trans. Power Syst.*, vol. 36, no. 6, pp. 4953–4966, 2021.
- [22] M. Farivar, L. Chen, and S. Low, "Equilibrium and dynamics of local voltage control in distribution systems," in *52nd IEEE Conference on Decision and Control (CDC)*, 2013, pp. 4329–4334.
- [23] R. D. Zimmerman, C. E. Murillo-Sanchez, and R. J. Thomas, "MATPOWER: Steady-State Operations, Planning, and Analysis Tools for Power Systems Research and Education," *IEEE Trans. Power Syst.*, vol. 26, no. 1, pp. 12–19, Feb. 2011.